Supplementary Material

Molecular dynamics study of wetting of alkanes on water: From high temperature to the supercooled region and the influence of second inflection points of interfacial tensions

Pauf Neupane and Gerald Wilemski

1 Contact angle using experimental interfacial tension values

The experimental interfacial tension for the octane-water and nonane-water systems are shown in Fig. S1.[1–3] These alkane-water interfacial tensions and the surface tension of pure liquids (water - Ref. [4] and alkane - Ref. [5]) were used to calculate the contact angle formed by octane and nonane on water as seen in Fig. S2. The values calculated using the alkane-water interfacial tension (γ_{aw}) values from Ref. [3] are consistently lower than those found using more reliable γ_{aw} values from Ref. [1] and Ref. [2] for the same alkane and temperature. Using the γ_{aw} values of Zeppieri *et al.*,[3] the contact angle can be calculated for the temperature range, 283-333 K, in the stable liquid region. The calculated contact angles are smaller than those found in our simulations, and in addition, for octane-water a transition to perfect wetting is found at 313 K. This temperature is considerably lower than the transition temperature 457 K (by extrapolation from Ref. [6]) or 484 K (by linear extrapolation of the high temperature spreading coefficients from Ref. [7]). As seen later in Fig. S9, it is also lower than the transition temperatures for pentane, hexane, and heptane, which casts further doubt on its reliabilty, even as an initial value.

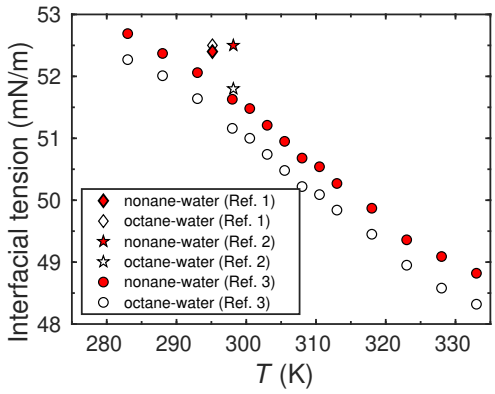

Fig. S1 The experimental interfacial tension of octane-water and nonane-water interfaces reported by Goebel and Lunkenheimer,[1] Mitrinović *et al.*,[2] and Zeppieri *et al.*[3]. The values reported in Ref. [3] are consistently lower than those reported in Refs. [1,2] for identical condition.

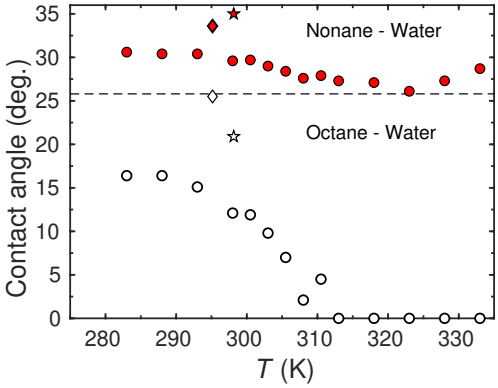

Fig. S2 The contact angle for nonane-water and octane-water systems calculated using experimental interfacial tension values for pure water,[4] alkane,[5] and alkane-water interfacial tension.[1–3] For alkane-water interfacial tensions, the symbols are consistent with Fig. S1. The dashed line separates the nonane-water and octane-water results.

Department of Physics, Missouri University of Science and Technology, Rolla, MO 65409, USA.
E-mail: pndz2@mst.edu
E-mail: wilemski@mst.edu

2 Effect of timestep and cutoff radius on interfacial tensions

We studied the dependence of the surface tension of PYS nonane on the LJ cutoff radius at 295 K and 225 K for different timesteps (1 fs, 2 fs and 5 fs) as seen in In Fig. S3. For all the LJ cutoff values studied, the tail corrected surface tension values for a 5 fs timestep were significantly lower ($\approx$ 6-10%) than those at 1 fs or 2 fs timesteps. On the other hand, the surface tension values calculated using 1 fs and 2 fs timesteps were found to be very close (differing by $< 2\%$). Hence, we chose to use a 2 fs timestep in our simulations. For all the timesteps studied, the tail corrected surface tension values were initially found to increase with the cutoff and become nearly constant at higher cutoff values ($\geq$ 1.75 nm). This behavior is consistent with the previous results for simple LJ liquids.[8–14]

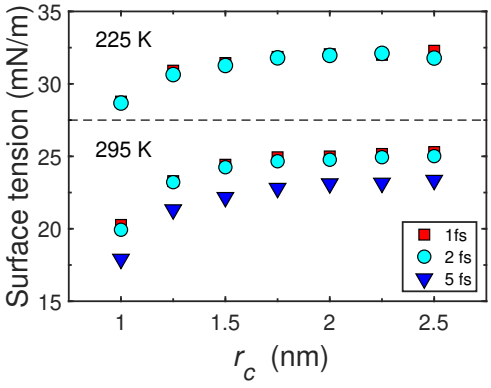

Fig. S3 The tail corrected surface tension values of PYS nonane as a function of LJ cutoff (r_c). The squares, triangles, and circles are for 1fs, 2fs, and 3 fs timestep, respectively. The dashed line separates the results for 225 K and 295 K.

We also studied the surface tensions of PYS octane, SPC/E water, and the PYS octane-SPC/E water interfacial tension for LJ cutoff radii ranging from 1.0 nm to 2.5 nm at 300 K temperature using 2 fs simulation timestep. The volume of the simulation boxes in our pure water as well as octane-water simulations were adjusted for higher cutoff values to satisfy the minimum image convention. A typical system with 2.5 nm cutoff consisted of 2680 water molecules in a $5.1 \times 5.1 \times 9.0$ nm^3 box or 550 octane plus 2680 water molecules in a box of dimensions $5.2 \times 5.2 \times 10.0$ nm^3. The cross-section of the octane-water simulation box was fixed and its length was allowed to fluctuate to accomodate barostatic fluctuations.

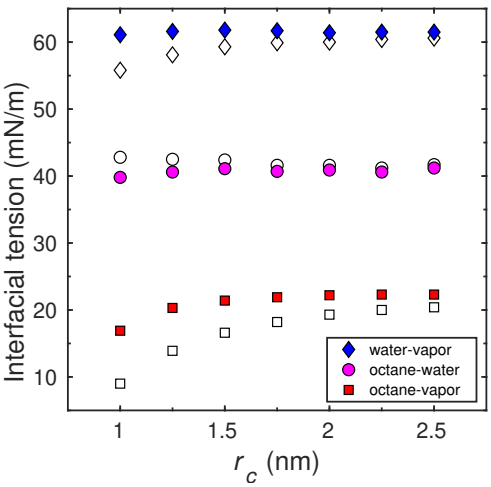

Fig. S4 Simulated surface tensions of SPC/E water (diamonds), PYS octane (squares) and the octane-water interfacial tensions (circles) plotted as a function of LJ cutoff (r_c) using 2fs timestep at 300 K. Filled markers account for the long range tail corrections to the interfacial tensions, while the open markers do not.

In Figure S4, the interfacial tensions are plotted versus the LJ cutoff radius (r_c). The filled and the open markers represent the respective interfacial tensions with and without including the long range tail correction (LRTC) γ_t. The surface tension of water and the octane-water interfacial tension ($\gamma + \gamma_t$) are found to be essentially independent of the cutoff radius unlike the case of octane. Octane behaved in a similar fashion as nonane as described above. The r_c dependence of SPC/E water is consistent with the TIP4P/2005

water result reported in Ref. [14]. Hence, we decided to use r_c = 1.75 nm for pure alkanes, and r_c = 1.5 nm for pure water and the alkane-water systems in our simulations at different temperatures as a compromise between accuracy and computational time.

The contribution of the LRTC γ_t should be included to ensure accurate determination of the interfacial tensions from MD simulations. Even at the highest cutoff value studied, the contributions of γ_t to the total surface tension of octane and water are found to be roughly 9% and 2%, respectively. The contribution of γ_t is higher for smaller r_c values. It is interesting to note that, with the optimized ε_{oc}, σ_{oc} values for the octane-water interaction in our simulations, the uncorrected interfacial tensions are found to be overestimated, and the tail correction values are negative. The negative tail correction is due to not using geometric mean rule (Berthelot rule) in determining ε_{oc}. With the geometric mean rule for ε_{oc}, γ_t would be 0.1 mN/m instead of -1.3 mN/m at the 1.5 nm cutoff value. (Of course, γ itself would also be quite different.)

3 Density profiles

The density profiles for TIP4P/2005 water and PYS nonane are plotted in Fig. S5 for 220 K, 400 K, and 500 K temperatures. In Fig. S6, the density profiles for the nonane-TIP4P/2005 water system at temperatures 220 K and 500 K are shown. All the low temperature density profiles contain an apophysis.

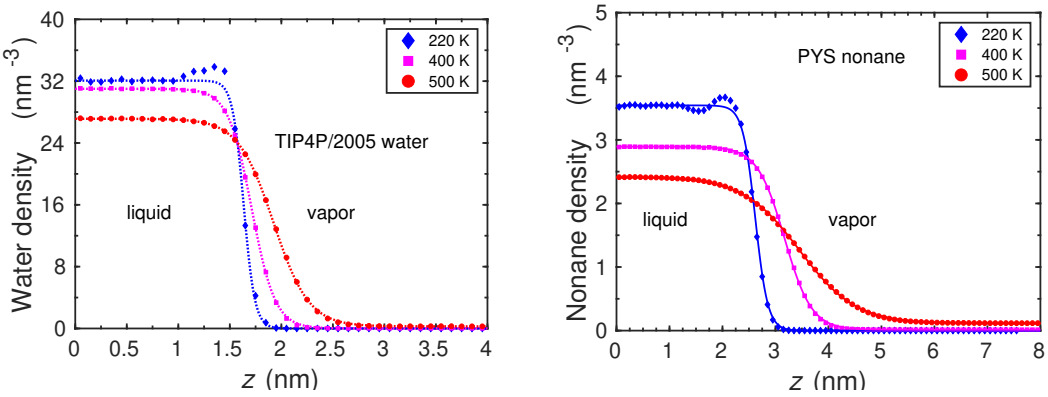

Fig. S5 Number density profiles of TIP4P/2005 water (upper) and PYS nonane (lower) plotted for different temperatures. Points are the densities calculated using bin size of 0.1 nm. Dotted and solid lines are the fitted density profiles.

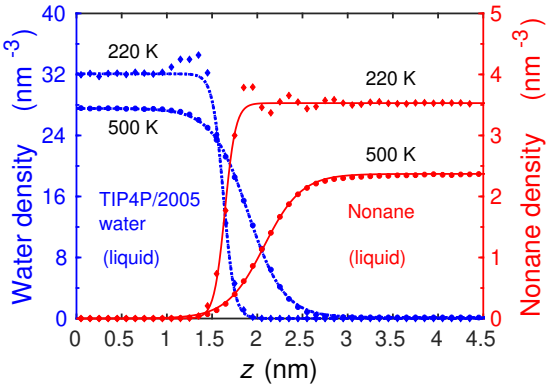

Fig. S6 Number density profiles of TIP4P/2005 water and PYS nonane in the nonane-water system at 220 K (diamonds) and at 500 K (circles) temperatures. Points are the densities calculated using bin size of 0.1 nm. The fitted profiles for water and nonane are represented by the dotted and solid lines, respectively.

4 The difference of the vapor-water and alkane-water interfacial tensions ($\gamma_w - \gamma_{aw}$)

In this work, the wetting behavior of PYS alkane on two different water models (SPC/E water and TIP4P/2005 water) was studied. For the same alkane, the behavior of the spreading coefficient (S) depends on the behavior of $\gamma_w - \gamma_{aw}$. Hence, the difference in the slopes of the S versus T curves for octane-SPC/E water and octane-TIP4P/2005 water is due to the differences in the slopes of $\gamma_w - \gamma_{aw}$ versus T curves for SPC/E water and TIP4P/2005 water.

The difference of the vapor-water and alkane-water interfacial tensions ($\gamma_w - \gamma_{aw}$) are shown in Figs. S7 and S8.

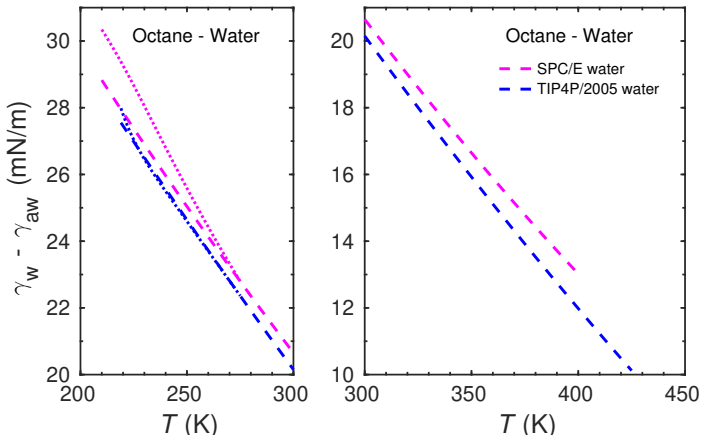

Fig. S7 The differences of vapor-water and octane-water interfacial tensions plotted versus temperature. The magenta lines are for SPC/E water and blue lines are for TIP4P/2005 water. Dotted lines include the SIP effect; dashed lines exclude it.

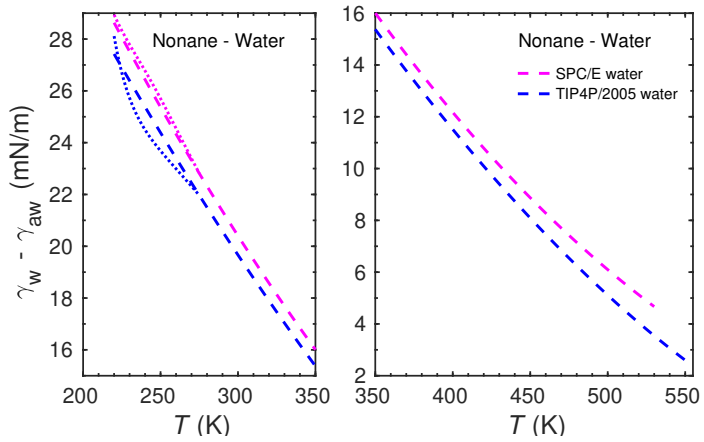

Fig. S8 The difference of vapor-water and nonane-water interfacial tensions plotted versus temperature. The magenta lines are for SPC/E water and blue lines are for TIP4P/2005 water. Dotted lines include the SIP effect; dashed lines exclude it.

5 Wetting transition temperatures

The wetting transition temperatures (T_w) for pentane, hexane and heptane on water were previously presented in Ref. [6]. Here, these T_w values are extrapolated to estimate the T_w values for octane and nonane on water. The wetting transition temperatures, T_w, for n-alkanes on water are shown in Fig. S9.

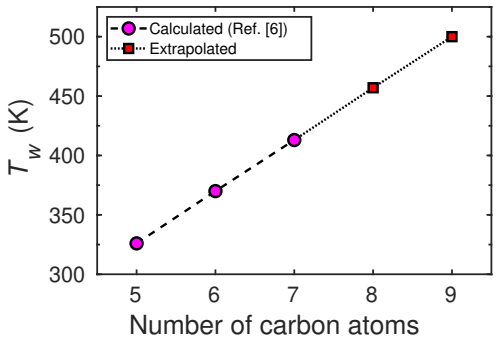

Fig. S9 Wetting transition temperature, T_w, plotted versus number of carbon atoms (n) in n-alkane. The filled squares are the extrapolated values based on previously calculated[6] T_w values for pentane, hexane and heptane (filled circles).

6 Error Analysis

The uncertainties in the interfacial tension values ($\delta\gamma_w$, $\delta\gamma_a$, $\delta\gamma_{aw}$) are determined using the standard errors[15] of the mean obtained from 3-8 simulation runs at each temperature. These $\delta\gamma_w$, $\delta\gamma_a$, and $\delta\gamma_{aw}$ are then propagated to calculate the uncertainties associated with the spreading coefficient (S) and the contact angle (θ_c) as

$$\delta S = \sqrt{\delta\gamma_w^2 + \delta\gamma_a^2 + \delta\gamma_{aw}^2}, \tag{1}$$

$$\delta\theta_c = \frac{\sqrt{\gamma_w^2\delta\gamma_w^2 + (\gamma_{aw}\cos\theta + \gamma_a)^2\delta\gamma_a^2 + (\gamma_a\cos\theta_c + \gamma_{aw})^2\delta\gamma_{aw}^2}}{\gamma_a\gamma_{aw}\sin\theta_c}, \qquad \theta_c \neq 0. \tag{2}$$

The numerical values (uncertainities) of the interfacial tension, spreading coefficient, and contact angle are given in Table S1-S5. The interfacial tensions γ_w, γ_a and γ_{aw} are tail corrected, and they are used to calculate the contact angle θ_c. In Table S5, γ_{w0}, γ_{a0} and γ_{aw0} are the interfacial tensions that do not include the tail correction and are used to calculate θ_{c0}. For the cases where $\cos\theta_c > 1$, which is unphysical, we assigned $\theta_c = 0$.

Table S1 Octane-SPC/E Water

T (K)	γ_w (mN/m)	γ_a (mN/m)	γ_{aw} (mN/m)	S (mN/m)	θ_c (deg.)
210	75.8 (0.5)	31.5 (0.1)	45.3 (0.3)	-1.0 (0.6)	18.9 (5.5)
215	74.8 (0.4)	30.6 (0.1)	44.9 (0.2)	-0.7 (0.5)	16.4 (5.1)
220	73.6 (0.2)	30.0 (0.2)	44.6 (0.4)	-1.0 (0.5)	19.2 (4.6)
225	72.8 (0.4)	29.6 (0.2)	44.4 (0.3)	-1.2 (0.5)	20.8 (4.8)
232.5	72.0 (0.2)	28.9 (0.1)	44.3 (0.4)	-1.2 (0.5)	21.4 (3.9)
240	70.7 (0.2)	27.8 (0.2)	43.7 (0.4)	-0.8 (0.5)	18.0 (5.7)
250	69.2 (0.1)	27.0 (0.1)	43.3 (0.3)	-1.1 (0.3)	20.5 (3.1)
262.5	67.1 (0.2)	25.7 (0.1)	42.8 (0.2)	-1.4 (0.3)	24.0 (2.4)
275	65.2 (0.1)	24.3 (0.1)	42.4 (0.2)	-1.5 (0.2)	25.2 (1.9)
287.5	63.5 (0.1)	23.2 (0.1)	41.6 (0.2)	-1.3 (0.2)	23.5 (2.4)
300	61.8 (0.1)	21.9 (0.1)	41.1 (0.1)	-1.2 (0.2)	23.8 (1.5)
312.5	59.6 (0.1)	20.6 (0.1)	40.1 (0.1)	-1.1 (0.2)	22.9 (1.6)
325	57.6 (0.1)	19.4 (0.1)	38.8 (0.1)	-0.6 (0.2)	18.2 (2.1)
337.5	55.9 (0.1)	18.2 (0.1)	38.1 (0.1)	-0.4 (0.2)	14.8 (2.7)
350	53.5 (0.1)	17.0 (0.1)	37.0 (0.1)	-0.5 (0.2)	17.0 (3.0)
362.5	51.4 (0.1)	15.9 (0.1)	35.7 (0.2)	-0.2 (0.2)	10.1 (6.8)
375	49.2 (0.1)	14.7 (0.1)	34.3 (0.2)	0.2 (0.2)	0.0
387.5	47.0 (0.1)	13.5 (0.1)	33.1 (0.1)	0.4 (0.2)	0.0
400	44.6 (0.1)	12.4 (0.1)	31.6 (0.2)	0.6 (0.2)	0.0

Table S2 Nonane-SPC/E Water (ε_{oc} = 0.65 kJ/mol)

T (K)	γ_w (mN/m)	γ_a (mN/m)	γ_{aw} (mN/m)	S (mN/m)	θ_c (deg.)
220	73.6 (0.2)	32.1 (0.1)	45.0 (0.7)	-3.5 (0.7)	35.2 (3.6)
225	72.8 (0.4)	31.7 (0.1)	44.8 (0.1)	-3.7 (0.4)	36.3 (2.1)
250	69.2 (0.1)	29.1 (0.1)	43.4 (0.2)	-3.3 (0.2)	35.4 (1.3)
275	65.2 (0.1)	26.6 (0.1)	42.6 (0.1)	-4.0 (0.2)	40.3 (0.9)
300	61.8 (0.1)	24.2 (0.1)	41.2 (0.2)	-3.6 (0.2)	39.6 (1.3)
325	57.6 (0.1)	21.7 (0.1)	39.6 (0.1)	-3.7 (0.2)	41.9 (1.0)
350	53.5 (0.1)	19.3 (0.1)	37.5 (0.1)	-3.3 (0.2)	41.5 (1.1)
375	49.2 (0.1)	17.2 (0.1)	35.3 (0.2)	-3.3 (0.2)	43.6 (1.6)
400	44.6 (0.1)	14.9 (0.1)	32.3 (0.1)	-2.6 (0.2)	41.2 (1.3)
425	39.8 (0.1)	12.8 (0.1)	29.5 (0.1)	-2.5 (0.2)	43.3 (1.5)
450	34.9 (0.1)	10.7 (0.1)	26.2 (0.2)	-2.0 (0.2)	41.9 (2.5)
475	29.8 (0.1)	8.5 (0.1)	22.4 (0.1)	-1.1 (0.2)	34.4 (2.7)
500	24.4 (0.1)	6.2 (0.1)	18.4 (0.1)	-0.2 (0.2)	16.9 (7.3)
525	19.1 (0.1)	4.3 (0.1)	14.1 (0.2)	0.7 (0.2)	0.0

Table S3 Octane-TIP4P/2005 Water

T (K)	γ_w (mN/m)	γ_a (mN/m)	γ_{aw} (mN/m)	S (mN/m)	θ_c (deg.)
220	81.8 (1.0)	30.0 (0.2)	54.1 (0.8)	-2.3 (1.3)	28.1 (7.9)
225	79.6 (0.8)	29.6 (0.2)	52.3 (0.8)	-2.3 (1.1)	28.2 (7.1)
232.5	78.4 (0.2)	28.9 (0.1)	52.4 (0.5)	-2.9 (0.5)	32.2 (3.0)
240	76.4 (0.4)	27.8 (0.2)	50.9 (0.5)	-2.3 (0.7)	29.3 (4.2)
250	75.0 (0.4)	27.0 (0.1)	50.7 (0.2)	-2.7 (0.5)	31.6 (2.7)
262.5	73.6 (0.1)	25.7 (0.1)	49.9 (0.3)	-2.0 (0.3)	27.9 (2.3)
275	71.8 (0.2)	24.3 (0.1)	49.3 (0.2)	-1.8 (0.3)	27.0 (2.3)
287.5	70.3 (0.1)	23.2 (0.1)	49.0 (0.2)	-1.9 (0.2)	27.9 (1.8)
300	68.3 (0.1)	21.9 (0.1)	48.3 (0.1)	-1.9 (0.2)	29.1 (1.3)
312.5	66.3 (0.1)	20.6 (0.1)	47.1 (0.1)	-1.4 (0.2)	25.2 (1.6)
325	64.5 (0.1)	19.4 (0.1)	46.4 (0.2)	-1.3 (0.2)	25.5 (2.3)
337.5	62.1 (0.1)	18.2 (0.1)	45.3 (0.1)	-1.4 (0.2)	26.8 (1.6)
350	60.3 (0.1)	17.0 (0.1)	44.1 (0.1)	-0.8 (0.2)	20.9 (2.2)
362.5	57.9 (0.1)	15.9 (0.1)	43.3 (0.1)	-1.3 (0.2)	26.9 (1.8)
375	55.7 (0.1)	14.7 (0.1)	41.8 (0.1)	-0.8 (0.2)	21.7 (2.4)
387.5	53.5 (0.2)	13.5 (0.1)	40.5 (0.1)	-0.5 (0.2)	18.1 (4.4)
400	50.8 (0.1)	12.4 (0.1)	38.9 (0.1)	-0.5 (0.2)	19.2 (3.1)
412.5	48.6 (0.1)	11.2 (0.1)	37.6 (0.1)	-0.2 (0.2)	12.3 (5.3)
425	46.1 (0.1)	10.1 (0.1)	35.8 (0.1)	0.2 (0.2)	0.0

Table S4 Nonane-TIP4P/2005 Water

T (K)	γ_w (mN/m)	γ_a (mN/m)	γ_{aw} (mN/m)	S (mN/m)	θ_c (deg.)
220	81.8 (1.0)	32.1 (0.1)	53.9 (0.8)	-4.2 (1.3)	37.2 (5.7)
225	79.6 (0.8)	31.7 (0.1)	52.7 (0.4)	-4.8 (0.9)	40.1 (3.8)
250	75.0 (0.4)	29.1 (0.1)	51.7 (0.3)	-5.8 (0.5)	45.6 (2.0)
275	71.8 (0.2)	26.6 (0.1)	50.0 (0.2)	-4.8 (0.3)	42.9 (1.3)
300	68.3 (0.1)	24.2 (0.1)	48.8 (0.2)	-4.7 (0.2)	44.0 (1.1)
325	64.5 (0.1)	21.7 (0.1)	46.8 (0.2)	-4.0 (0.2)	42.4 (1.3)
350	60.3 (0.1)	19.3 (0.1)	44.6 (0.2)	-3.6 (0.2)	42.2 (1.4)
375	55.7 (0.1)	17.2 (0.1)	42.0 (0.1)	-3.5 (0.2)	43.8 (1.1)
400	50.8 (0.1)	14.9 (0.1)	39.4 (0.1)	-3.5 (0.2)	46.6 (1.1)
425	46.1 (0.1)	12.8 (0.1)	36.6 (0.1)	-3.3 (0.2)	48.4 (1.2)
450	40.8 (0.1)	10.7 (0.1)	32.8 (0.1)	-2.7 (0.2)	47.5 (1.5)
475	35.4 (0.1)	8.5 (0.1)	29.3 (0.1)	-2.4 (0.2)	49.7 (1.7)
500	29.9 (0.1)	6.2 (0.1)	24.9 (0.1)	-1.2 (0.2)	40.3 (2.8)
525	24.2 (0.1)	4.3 (0.1)	20.2 (0.1)	-0.3 (0.2)	23.7 (6.8)
550	15.8 (0.2)	2.5 (0.1)	18.5 (0.1)	0.2 (0.2)	0.0

Table S5 Nonane-SPC/E Water (ε_{oc} = 0.66 kJ/mol)

T (K)	γ_w (mN/m)	γ_a (mN/m)	γ_{aw} (mN/m)	θ_c (deg.)	γ_{w0} (mN/m)	γ_{a0} (mN/m)	γ_{aw0} (mN/m)	θ_{c0} (deg.)
220	73.6 (0.2)	32.1 (0.1)	43.6 (0.6)	27.4 (4.1)	71.0(0.2)	27.2 (0.1)	44.8 (0.6)	19.7 (6.3)
250	69.2 (0.1)	29.1 (0.1)	42.6 (0.1)	30.9 (1.1)	66.7 (0.1)	24.5 (0.1)	44.0 (0.1)	27.5 (1.3)
275	65.2 (0.1)	26.6 (0.1)	41.6 (0.3)	35.0 (1.9)	62.7 (0.1)	22.2 (0.1)	43.0 (0.3)	34.3 (2.2)
300	61.8 (0.1)	24.2 (0.1)	40.3 (0.1)	34.4 (1.1)	59.3 (0.1)	20.1 (0.1)	41.7 (0.1)	35.0 (1.2)
325	57.6 (0.1)	21.7 (0.1)	38.3 (0.2)	33.9 (1.7)	55.2 (0.1)	17.9 (0.1)	39.7 (0.2)	36.0 (1.8)
350	53.5 (0.1)	19.3 (0.1)	36.4 (0.1)	34.0 (1.3)	51.3 (0.1)	15.8 (0.1)	37.7 (0.1)	36.2 (1.4)

References

1 A. Goebel and K. Lunkenheimer, *Langmuir*, 1997, **13**, 369–372.

2 D. M. Mitrinović, A. M. Tikhonov, M. Li, Z. Huang and M. L. Schlossman, *Phys. Rev. Lett.*, 2000, **85**, 582.

3 S. Zeppieri, J. Rodríguez and A. L. López de Ramos, *J. Chem. Eng. Data*, 2001, **46**, 1086–1088.

4 T. Petrova and R. B. Dooley, *Revised Release on Surface Tension of Ordinary Water Substance*, International Association for the Properties of Water and Steam (IAPWS), Moscow, Russia, 2014.

5 E. W. Lemmon, M. O. McLinden and D. G. Friend, "Thermophysical Properties of Fluid Systems", in *NIST Chemistry WebBook, NIST Standard Reference Database Number 69*, ed. P. J. Linstrom and W. G. Mallard, National Institute of Standards and Technology, Gaithersburg MD, 20899, 2020.

6 V. C. Weiss, *J. Chem. Phys.*, 2006, **125**, 084718.

7 S.-Y. Akatsuka, H. Yoshigiwa and Y. H. Mori, *J. Colloid Interface Sci.*, 1995, **172**, 335–340.

8 A. Trokhymchuk and J. Alejandre, *J. Chem. Phys.*, 1999, **111**, 8510–8523.

9 D. Duque and L. F. Vega, *J. Chem. Phys.*, 2004, **121**, 8611–8617.

10 F. J. Blas, L. G. MacDowell, E. de Miguel and G. Jackson, *J. Chem. Phys.*, 2008, **129**, 144703.

11 R. E. Isele-Holder, W. Mitchell and A. E. Ismail, *J. Chem. Phys.*, 2012, **137**, 174107.

12 F. Goujon, A. Ghoufi, P. Malfreyt and D. J. Tildesley, *J. Chem. Theory Comput.*, 2015, **11**, 4573–4585.

13 A. Ghoufi, P. Malfreyt and D. J. Tildesley, *Chem. Soc. Rev.*, 2016, **45**, 1387–1409.

14 L. Lundberg and O. Edholm, *J. Chem. Theory Comput.*, 2016, **12**, 4025–4032.

15 D. G. Altman and J. M. Bland, *BMJ*, 2005, **331**, 903.